States in ^{197}Pt populated by the (d,p), (d,t) and (n,γ) reactions*

Y. Yamazaki† and R. K. Sheline
Florida State University, Tallahassee, Florida 32306

E. B. Shera
Los Alamos Scientific Laboratory of the University of California, Los Alamos, New Mexico 87545

(Received 19 December 1977)

States in ^{197}Pt have been studied using the ^{196}Pt$(d,p)^{197}$Pt and ^{198}Pt$(d,t)^{197}$Pt reactions with 13.5 MeV deuterons and the ^{196}Pt(n,γ) reaction using thermal neutrons. The measured Q values were 3.606 ± 0.020, -1.221 ± 0.020, and 5.8463 ± 0.0004 MeV for the (d,p), (d,t), and (n,γ) reactions, respectively. Transferred l values have been determined from angular distributions and spectroscopic factors determined by comparison with distorted-wave Born-approximation calculations. Some of the states can be tentatively assigned as Nilsson states arising from an oblate deformation. These include the $5/2^-[532]$, decoupled $1/2^+[600]$ and $9/2^+[615]$ states. A number of low lying states with $l = 1$ cannot be explained using the Nilsson model or the shell model.

[NUCLEAR REACTIONS, NUCLEAR STRUCTURE ^{196}Pt(d,p), ^{198}Pt(d,t), E_d = 13.5 MeV. Measured $\sigma(E_p,\theta)$, $\sigma(E_t,\theta)$, Q, DWBA analysis; ^{196}Pt(n_{th},γ). Measured E_γ, I_γ, Q. Deduced energies, l, J, π of ^{197}Pt levels, enriched targets.]

I. INTRODUCTION

In this paper, we present the results of (d,p), (d,t), and (n,γ) experiments designed to study the nuclear structure of ^{197}Pt. This experiment is an extension of a previous experiment[1] in which the states of ^{195}Pt were studied by use of the (d,p) and (d,t) reactions.

Quadrupole moments of first excited 2^+ states in ^{194,196,198}Pt were measured previously by using the reorientation effect in Coulomb excitation and were found to be positive.[2] Anomalous rotational spectra built on a high-spin unique-parity $i_{13/2}$ state in the lighter odd platinum isotopes, studied by means of (HI, $xn\gamma$) reactions, were shown to form decoupled bands.[3] Both of these experiments indicate that the platinum isotopes have a (time averaged) oblate spheroidal shape.

In our recent study[1] of ^{195}Pt, the rotation-vibration model of Faessler and Greiner[4] was used to take into account the effects of the γ vibration. This model was reasonably successful in predicting the excitation energies and spectroscopic factors of the states in ^{195}Pt by assuming oblate deformation. It is of interest to see if the same rationale can be applied to an explanation of the states in ^{197}Pt.

Although several previous experiments[5] have been conducted on ^{197}Pt, only two excited states at 53 and 399 keV were studied in detail. The previous (d,p) and (d,t) reaction experiments were made with targets of low isotopic enrichment and with poor resolution.[6] Recently, the γ rays from the ^{197}Ir β^- decay were measured[5] and used to construct a decay scheme. However, no transition multipolarities were determined and no coincidence measurements were made. We have carried out the (d,p) and (d,t) experiments with ~96% enriched targets and with better resolution than previous experiments to determine the transferred l values and spectroscopic factors of the states in ^{197}Pt. In addition, a study of the thermal neutron capture γ rays of the ^{196}Pt$(n,\gamma)^{197}$Pt reaction is included in the present work.

II. EXPERIMENTAL PROCEDURES AND RESULTS OF ANALYSIS

A. The ^{196}Pt$(d,p)^{197}$Pt and ^{198}Pt$(d,t)^{197}$Pt reactions

The experimental procedure for the (d,p) and (d,t) reactions was essentially identical to that described in a previous paper.[1] Targets of thickness $\cong 50$ μg/cm^2 were prepared by the vacuum evaporation of samples of platinum metal, isotopically enriched to 97.5% in ^{196}Pt and 95.8% in ^{198}Pt onto $\cong 50$ μg/cm^2 carbon foils. A 13.5-MeV deuteron beam from the Florida State University (FSU) tandem Van de Graaff accelerator was used for both the ^{196}Pt$(d,p)^{197}$Pt and ^{198}Pt$(d,t)^{197}$Pt reactions. The reaction products were analyzed in the FSU Browne-Buechner type spectrograph[7] and detected photographically in 50-μm nuclear emulsions. Absolute Q values for the ^{196}Pt$(d,p)^{197}$Pt and ^{198}Pt$(d,t)^{197}$Pt reactions were determined with respect to the ^{12}C(d,p) and ^{16}O(d,p) reference reactions and to the ^{198}Pt(d,d) elastic scattering,

respectively.

The reaction products were observed at laboratory angles of 30°, 40°, 50°, 60°, 70°, 80°, and 100°. Typical spectra for the (d,p) and (d,t) reactions are shown in Fig. 1 and Fig. 2, respectively. The observed peaks had resolutions of 13 to 18 keV full width at half maximum (FWHM) depending on angle and Q value. The measured ground state Q values were $+3.606 \pm 0.020$ MeV and -1.221 ± 0.020 MeV for the ^{196}Pt$(d,p)^{197}$Pt and ^{198}Pt$(d,t)^{197}$Pt reactions, respectively. Although the former value is in good agreement with the value of $+3.625 \pm 0.003$ MeV listed in the mass table of Wapstra and Bos,[8] the latter value is considerably different from the mass table value of -1.304 ± 0.019 MeV.

The absolute cross sections were determined by assuming that the elastic scattering cross sections at 25° are the same as the distorted-wave Born-approximation (DWBA) predictions made with the optical model parameters of the previous paper.[1] A series of DWBA calculations was carried out using the computer code DWUCK [9] to determine transferred l values and spectroscopic factors. The observed angular distributions are compared with the theoretical angular distributions in Fig. 3 and Fig. 4. In computing the theoretical distributions, we assumed the transferred angular momenta j listed in Table I, since these values give the best agreement with the observed angular distributions. However, it is difficult to determine the values of j from the angular distributions and the listed values should only be considered as estimates.

The spectroscopic factor S is given by

$$\frac{d\sigma}{d\Omega} = 2NS\sigma^{l}_{\mathrm{DW}}(\theta) = 2NS\,\frac{\sigma^{j}_{\mathrm{DW}}(\theta)}{2j+1}\,, \tag{1}$$

where N is a normalization factor and $\sigma^{j}_{\mathrm{DW}}(\theta)$ is obtained from the DWBA calculation. Although the value of $\sigma^{j}_{\mathrm{DW}}(\theta)$ depends on the transferred angular momenta j, the value of $\sigma^{l}_{\mathrm{DW}}(\theta)$ defined in Eq. (1) is relatively independent of the value j. Thus, the spectroscopic factor S does not depend on the assumed transferred angular momenta j. Normalization factors $N = 1.53$ and $N = 3.33$ were used for the (d,p) and (d,t) reactions, respectively. The deduced spectroscopic factors and transferred l values are listed in Table I.

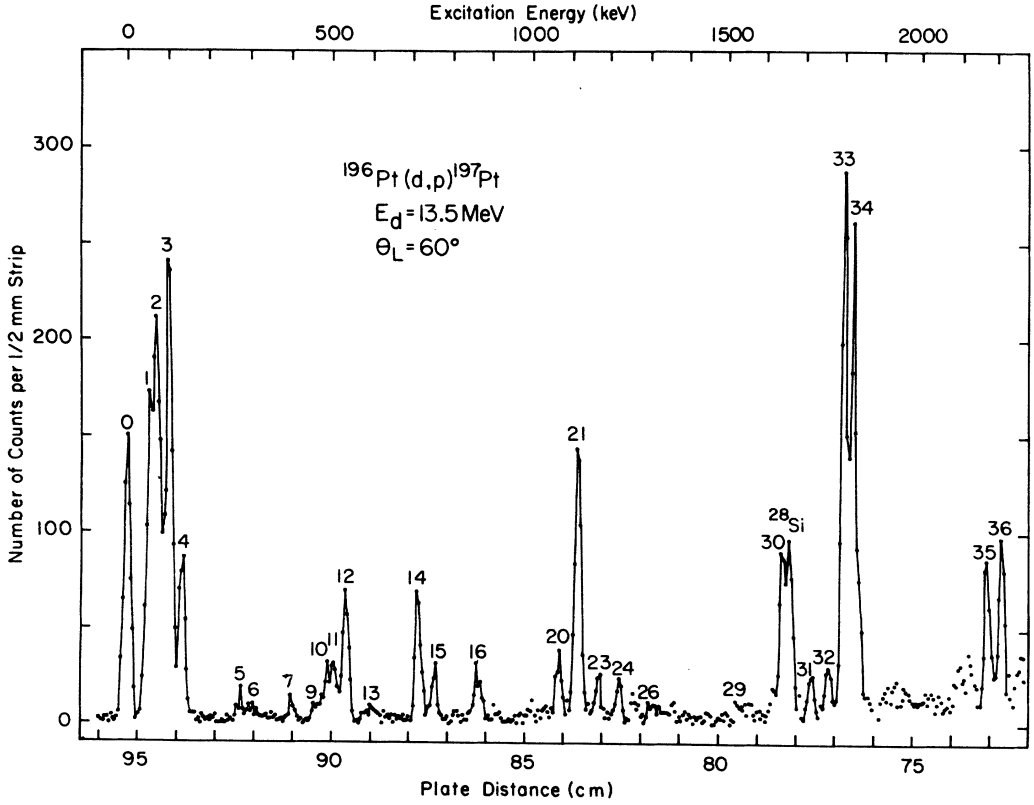

FIG. 1. Proton spectrum for the (d,p) reaction on ^{196}Pt at 60°.

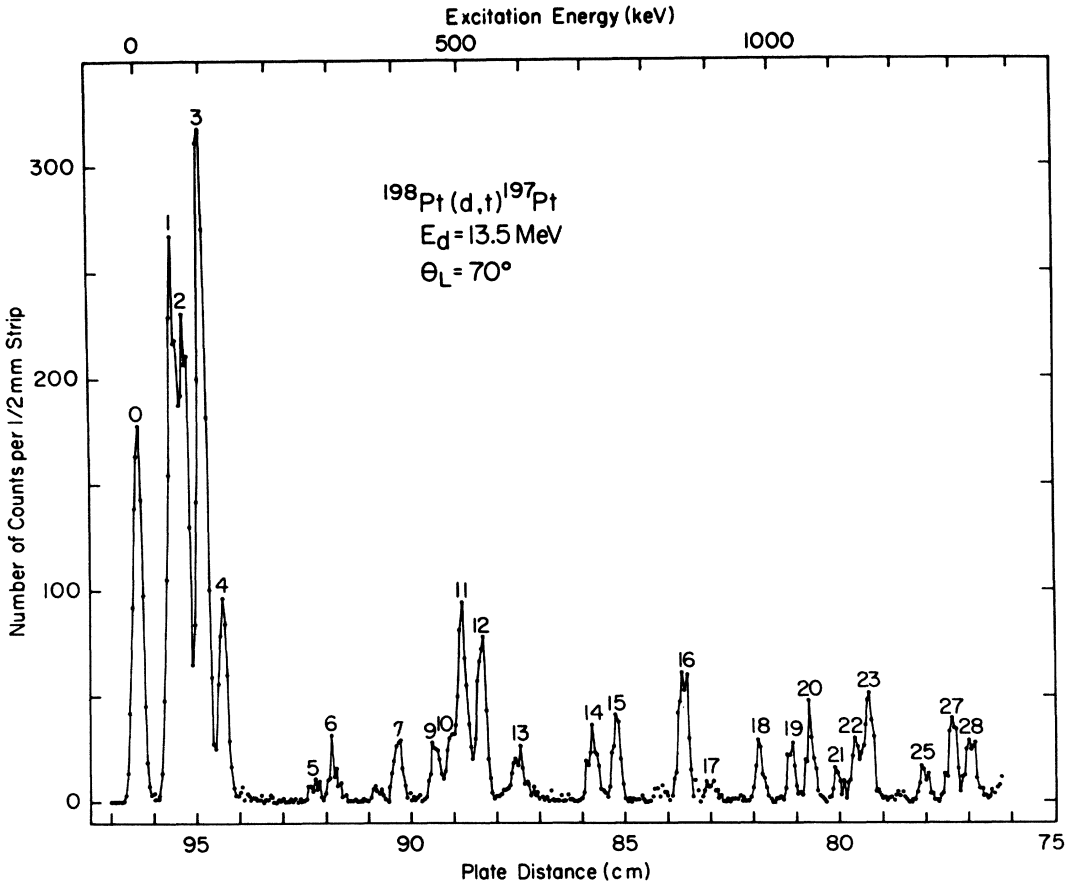

FIG. 2. Triton spectrum for the (d,t) reaction on ^{198}Pt at 70°.

B. The neutron capture γ experiment

The thermal neutron capture measurements were done using the Los Alamos neutron capture γ-ray facility. A 0.100 g sample of ^{196}Pt metallic powder (97.51% ^{196}Pt, 1.57% ^{195}Pt, 0.63% ^{194}Pt, and 0.29% ^{198}Pt) was mixed with graphite powder and formed into a target 0.9 cm in diameter and 0.1 cm in thickness. The arrangement of the target and detector is the same as that described in Ref. 10.

A Ge(Li) detector was placed at the center of a cylindrical NaI(Tl) annulus. Pulses from a preamplifier on the Ge(Li) detector were amplified with a Tennelec linear amplifier (TC205A) and analyzed with a Canberra 4092-channel analog to digital converter. For high-energy γ rays the Ge(Li) pulses into the ADC were gated by the occurrence of a pair of 511 keV pulses from the annulus. Thus, at high energies the system was used as a two-quantum escape pair spectrometer. For low-energy γ rays the detector system was operated as a total energy spectrometer (anti-coincidence mode). The ADC was stabilized by use of two reference peaks generated by a standard pulser.

For γ rays with energies below 1 MeV, the radiation from a mixed reference source consisting of ^{109}Cd, ^{57}Co, ^{139}Ce, ^{113}Sn, ^{137}Cs, ^{88}Y, and ^{60}Co was used as a calibration standard for both the energies and intensities. For the high-energy γ rays, the γ rays from the ^{14}N$(n,\gamma)^{15}$N were used as energy and intensity calibration standards.[11] The observed γ-ray intensities were corrected for absorption in the target.

Although the atomic percent of ^{195}Pt is only 1.57% in the target, many γ rays from the ^{195}Pt$(n,\gamma)^{196}$Pt reaction were among the prominent peaks in the spectra, since the thermal neutron captive cross section of ^{195}Pt is much larger than that of ^{196}Pt. These impurity γ rays were identified and eliminated by comparing the energies and intensities of the observed spectra with the results of recent measurements of the ^{195}Pt$(n,\gamma)^{196}$Pt reaction by Cizewski and Casten.[12] A delayed spectrum, recorded following neutron

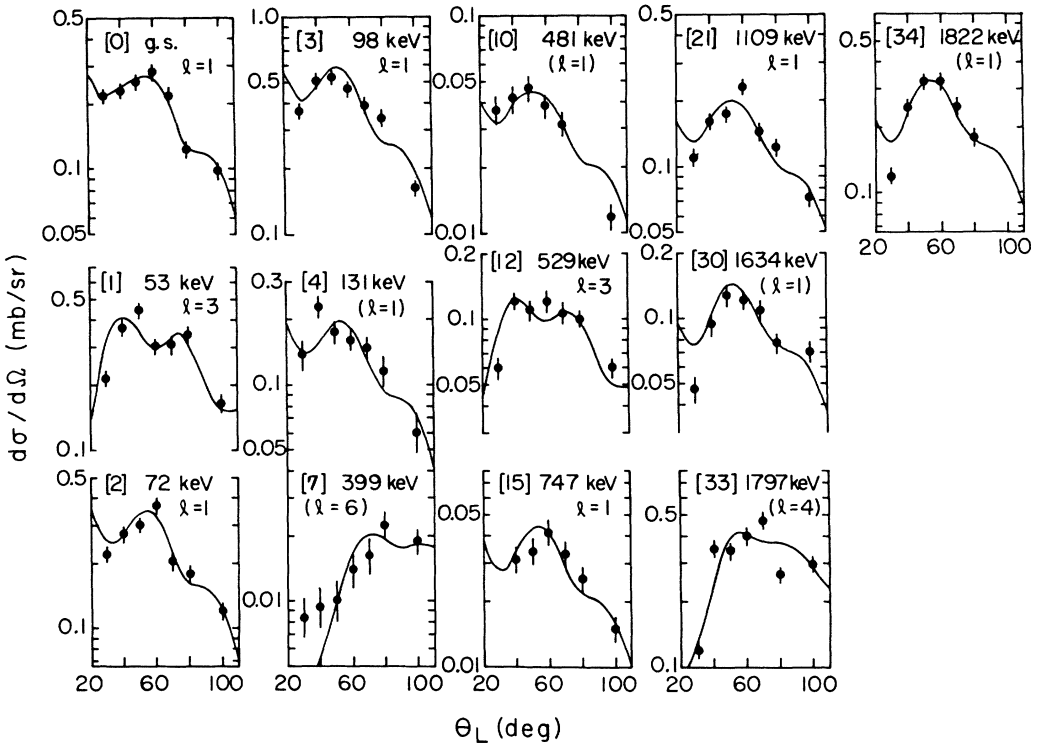

FIG. 3. Angular distributions for transitions in the ^{196}Pt $(d,p)^{197}$Pt reaction at 13.5 MeV. The curves are the results of the DWBA calculations.

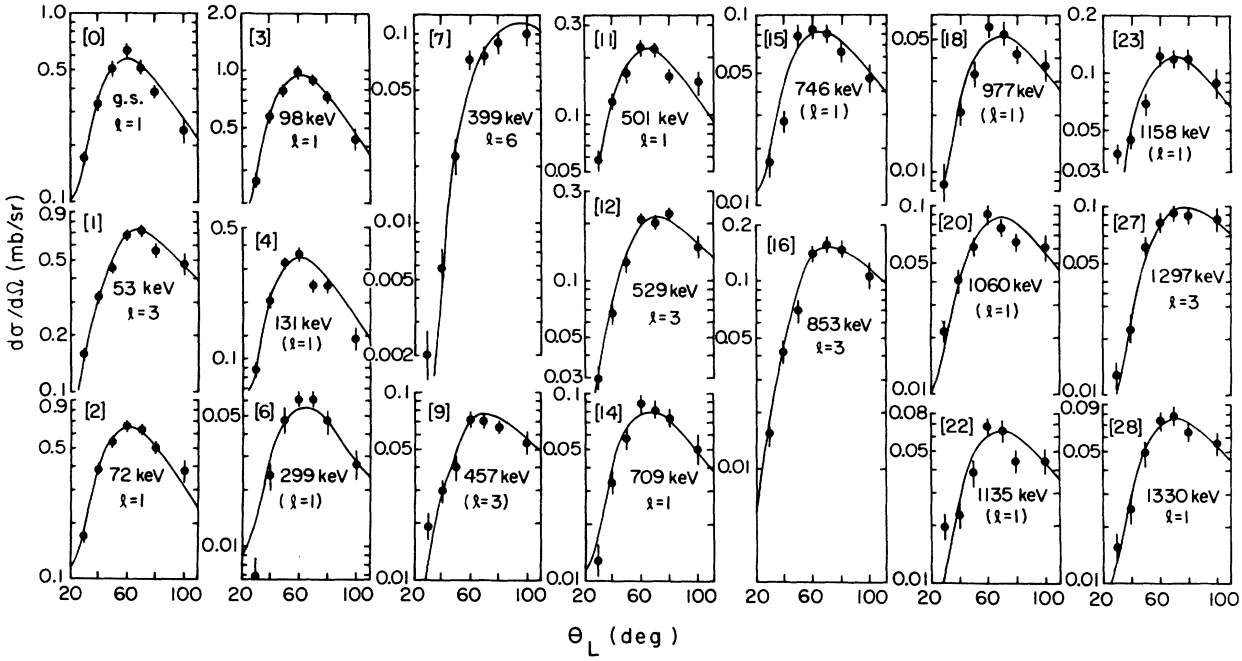

FIG. 4. Angular distributions for transitions in the ^{198}Pt$(d,t)^{197}$Pt reaction at 13.5 MeV. The curves are the results of the DWBA calculations.

TABLE I. States observed in ^{197}Pt. The assumed spins listed in the last column were used in determining the spectroscopic factors.

	Energy (keV)				l		Spectroscopic factor S		Assumed
	(d,p)	(d,t)	$HE(n,\gamma)$	$LE(n,\gamma)$	(d,p)	(d,t)	(d,p)	(d,t)	$J\pi$
0	0	0	0.0	0.0	1	1	0.13	0.21	$\frac{1}{2}^-$
1	53.2	52.4		53.11(7)	3	3	0.63	0.91	$\frac{5}{2}^-$
2	71.9	70.8		71.58(6)	1	1	0.14	0.21	$\frac{3}{2}^-$
3	98.4	97.8	98.5(4)	98.56(9)	1	1	0.24	0.33	$\frac{3}{2}^-$
4	130.9	130.1	130.4(5)	130.99(5)	(1)	(1)	0.08	0.13	$\frac{3}{2}^-$
5		268.2	269.1(3)	269.12(4)					
6		299.2		299.33(4)		(1)		0.02	$\frac{3}{2}^-$
7	398.5	399.2		399.6(2)[a]	(6)	6	0.30	1.40	$\frac{13}{2}^+$
8			425.7(2)						
9		457.3		456.80(6)		(3)		0.12	$\frac{5}{2}^-$
10	481.6	481.1			(1)		0.02		$\frac{1}{2}^-$
11	501.1	500.8	502.3(3)	502.44(5)		1		0.10	$\frac{1}{2}^-$
12	529.6	529.0			3	3	0.18	0.36	$\frac{5}{2}^-$
13		591.6		595.26(8)					
14	709.0	708.6	708.5(2)	708.36(5)		1	0.04	0.04	$\frac{3}{2}^-$
15	747.1	745.7	747.7(1)	747.81(11)	1	(1)	0.01	0.04	$\frac{3}{2}^-$
16		852.8				3		0.30	$\frac{5}{2}^-$
17		897.0							
18		976.5	977.9(6)	977.9(2)		(1)		0.03	$\frac{3}{2}^-$
19		1029							
20		1060				(1)		0.06	$\frac{1}{2}^-$
21	1109	1105			1		0.07		$\frac{1}{2}^-$
22		1135				(1)		0.05	$\frac{1}{2}^-$
23	1159	1158				(1)		0.09	$\frac{1}{2}^-$
24	1214								
25		1249							
26	1290								
27		1297				3		0.27	$\frac{5}{2}^-$
28		1330				1		0.07	$\frac{1}{2}^-$
29	1516								
30	1634				(1)		0.04		$\frac{3}{2}^-$
31	1706								
32	1754								
33	1797				(4)		1.35		$\frac{9}{2}^+$
34	1822				(1)		0.09		$\frac{3}{2}^-$
35	2176								
36	2214								

[a]Determined from delayed 346.5(1) keV γ ray.

irradiation of the target, was used to identify the γ rays from ^{197}Au which occurred in the prompt (n,γ) spectrum due to the metastable 399.5 keV state and to the ground state of ^{197}Pt both of which decay to ^{197}Au.

The observed high-energy and low-energy γ rays assigned to ^{197}Pt are listed in Tables II and III, respectively. The 5577 and 5099 keV γ rays had been previously assigned[13] to ^{196}Pt. However, the ratios of the intensity of these γ rays to those of the 5255 keV γ ray from the ^{195}Pt$(n,\gamma)^{196}$Pt (0.39 and 3.9 in the enriched target, and 0.03 and 0.20 in the natural target[13]) indicate that it is most reasonable to assign these two transitions to

TABLE II. High-energy thermal neutron capture γ rays from $^{196}Pt(n,\gamma)^{197}Pt$.

Energy (keV)	Intensity (Rel.)	Excitation energy (keV)
5846.3(4)	107(9)	0.0
5747.8(6)	2.7(6)	98.5(4)
5715.9(7)	8.2(19)	130.4(5)
5577.2(5)	10(2)	269.1(3)
5420.6(5)	6.2(9)	425.7(2)
5344.0(5)	3.9(9)	502.3(3)
5137.8(4)	17(2)	708.5(2)
5098.5(4)	≡100	747.7(1)
4868.4(8)	18(3)	977.9(6)

^{197}Pt. The 131 and 269 keV γ-ray lines observed in the prompt spectrum are contaminated to some extent by lines of these approximate energies which arise in the decay of ^{197}Au. The energies and intensities of the prompt lines listed in Table III have been corrected for this contamination.

III. DISCUSSION

A. Level structure

All of the states below 1 MeV observed in the (d,p) or (d,t) reactions and in the high-energy neutron capture γ rays are shown in Fig. 5. The excitation energies obtained by assuming that the high-energy γ rays are primary transitions correspond well to those obtained from the (d,p) or (d,t) reactions. In all cases where they were determined, the assigned l values of the states also fed directly by high-energy capture γ rays were $l=1$. This agreement supports the proposed l-value assignments since it is well known that the direct high-energy (n,γ) spectrum is dominated by dipole transitions.

The low-energy γ rays were placed in the decay scheme shown in Fig. 5 by use of the Ritz combination principle. The energy-loop discrepancies of the level scheme are consistently less than the experimental uncertainties. Another requirement to be satisfied by the decay scheme is that the transition intensities into and out of each state balance. However, to compute the intensities precisely the multipolarities and mixing ratios of the transitions must be known in order to calculate conversion coefficients. Such information can only be estimated in most cases. Other intensity ambiguities arise from the possible presence of unassigned γ rays whose energies are above 750

TABLE III. Low-energy thermal neutron capture γ rays from $^{196}Pt(n,\gamma)^{197}Pt$. The γ rays with a symbol X are placed in level scheme. The γ ray with a symbol XX is placed twice.

	Energy (keV)	Intensity (Rel.)		Energy (keV)	Intensity (Rel.)
X	71.53(17)	88(39)		453.70(22)	1.9(7)
X	98.58(10)	30(28)	X	456.81(6) [b]	18(2)
X	130.99(5)	11(5)	X	502.44(5)	31(2)
	135.21(4) [a]	25(10)		517.11(5)	20(2)
X	138.13(4)	19(8)	X	523.77(7)	11(1)
X	157.38(19) [b]	2.4(12)		527.18(15) [a]	2.7(6)
	167.32(15)	9.8(31)	X	542.22(9) [d]	11(1)
X	216.05(7)	11(2)		558.42(6)	16(2)
X	227.62(15) [c]	4.0(15)		570.65(20)	2.0(5)
X	233.27(13)	3.7(12)	X	578.31(14)	8.2(15)
X	246.15(15) [b]	8.9(24)	X	595.17(11)	5.9(10)
	259.25(11)	2.4(10)		620.10(13)	3.8(6)
X	269.12(4) [c]	59(5)		625.50(6)	15(2)
	274.08(4) [d]	29(3)	X	636.73(10)	6.2(9)
X	299.34(4) [b]	19(2)	X	649.22(5)	≡100
X	371.45(34)	2.6(15)		658.74(18)	3.5(8)
	390.38(17)	3.5(8)	X	676.12(14)	3.1(5)
XX	404.03(10) [b]	1.7(6)	X	695.04(21)	3.9(7)
X	430.89(5) [c]	20(2)		701.93(12)	5.6(6)
X	439.35(10)	6.8(9)	X	708.35(5) [d]	36(2)
	441.81(9)	8.7(11)			

[a] Placed in the ^{197}Ir β^- decay scheme (Ref. 5). Not placed in the present decay scheme.
[b] Placed in the ^{197}Ir β^- decay scheme (Ref. 5) in the same way as present.
[c] Placed in the ^{197}Ir β^- decay scheme (Ref. 5) in a different way from the present decay scheme.
[d] Observed in the work of Ref. 5 but not placed in the ^{197}Ir β^- decay scheme.

keV. In view of these uncertainties we find no intensity balance inconsistencies in the proposed level scheme of Fig. 5.

It is also possible to test the consistency of the proposed level scheme by comparing the γ-ray intensities observed from the ^{197}Ir β^- decay and those of the (n,γ) reaction, since the ratio of intensities of the transitions depopulating a given state should be the same for both experiments. The assignments of γ rays shown with solid lines in Fig. 5 satisfy this condition. The 227.6, 269.1, 430.9, 542.2, and 708.4 keV γ rays observed in both of the experiments (see the footnotes of Table III) were placed by the author of Ref. 5 in different ways from the present level scheme. The 227.6 keV γ ray was previously assigned to depopulate the 684.7 keV state together with the 496.4 keV γ ray. Although the intensity of the 496.4 keV transition is about ten times of that of the 227.6 keV transition in the decay experiment, the 496.4 keV transition was not observed in the present (n,γ) experiment. However, the assignment of the 227.6 keV, γ ray to the 299.3 keV state, as shown in Fig. 5, is consistent with the transition intensities observed in both experiments. Similarly, the assignment of the 269.1 keV γ ray has been changed since its previous placement is inconsistent with the present experiment. Also, the previously unassigned 708.4 keV γ ray is assigned in the present work to the 708.4 keV state. The other transitions associated with the 269.1 and 708.4 keV γ rays in the proposed level scheme were not observed previously presumably because of their weak intensities. When the previous assignments of the 227.6, 269.1, and 496.4 keV γ rays are changed, the existence of the proposed states at 188.2 and 684.7 keV become questionable and these states are not included in the present level scheme. Our proposed assignments for the 430.9 and 542.2 keV γ rays, shown with the dotted lines in Fig. 5, are to be considered very tentative, since the other strong γ rays associated with these transitions were not observed in the beta decay study.

B. Interpretation of level structure

The nature of the low-lying states in ^{195}Pt has been described[1] with reasonable success in terms

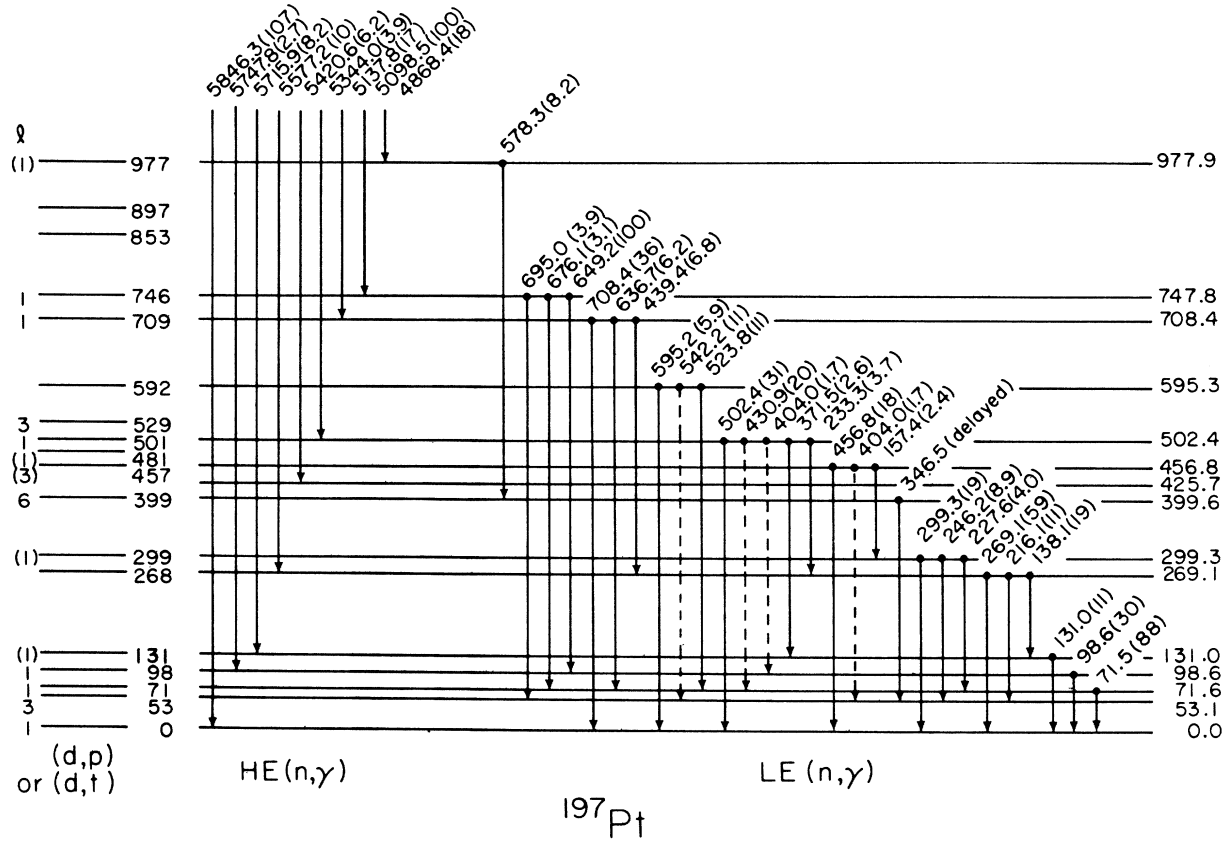

FIG. 5. The states in ^{197}Pt below 1 MeV observed in the present (d,p), (d,t), and (n,γ) reactions. The energy is given in keV and numbers in parentheses are relative γ-ray intensities. Dashed lines are γ rays placed tentatively.

of the rotation-vibration model[4] by assuming an oblate nuclear deformation ($\beta \cong -0.13$ and $\langle\gamma^2\rangle^{1/2} \cong 30°$). In spite of extreme shape fluctuation indicated by the value $\langle\gamma^2\rangle^{1/2} \cong 30°$ the Nilsson model[14] was found to be reasonably valid for states below 600 keV.[1] These states were assigned as members of the $\frac{1}{2}^-[530]$, $\frac{3}{2}^-[532]$, $\frac{5}{2}^-[532]$, $\frac{3}{2}^-[541]$, and decoupled $\frac{1}{2}^+[600]$ bands. In addition, the head of the $\frac{9}{2}^+[615]$ band was identified with a state at 1889 keV which has a spectroscopic factor $S(d,p) = 0.85$. A similar attempt has been made to describe the observed states in ^{197}Pt in terms of the Nilsson model. To assist in making Nilsson assignments a comparison between the states in ^{195}Pt and those in ^{197}Pt is shown in Fig. 6. It should be noted that we have used the oblate asymptotic quantum numbers ($Nn_z\Lambda$) (Ref. 15) to label the Nilsson states as in Ref. 1 and Ref. 16 rather than the prolate asymptotic quantum numbers that were used in Ref. 17.

The spin parities of the ground state and 53 keV state in ^{197}Pt were previously assigned as $\frac{1}{2}^-$ and $\frac{5}{2}^-$, respectively.[5] The observed l values are $l=1$ and $l=3$, respectively, supporting the previous assignments. Since the spectroscopic factors determined for the $\frac{5}{2}^-$ state are similar to those of the 130 keV state of ^{195}Pt as shown in Fig. 6, the $\frac{5}{2}^-$ state is assigned as the $\frac{5}{2}^-[532]$ band head.

The state at 399 keV, assigned in Ref. 5 as $\frac{13}{2}^+$, was observed in both the (d,p) and (d,t) reactions. The $l=6$ value for the transferred neutron supports the previous spin assignment. The (d,t) spectroscopic factor $S(d,t) = 1.40$ is very close to the value 1.58 of the $\frac{13}{2}^+$ state in ^{195}Pt. The smaller (d,p) spectroscopic factor and higher excitation energy (see Fig. 6) are reasonable because the Fermi level is probably higher in ^{197}Pt. The state observed at 1797 keV in ^{197}Pt has the spectroscopic factor $S(d,p) = 1.35$ with $l=(4)$, and presumably corresponds to the $\frac{9}{2}^+[615]$ band head at 1899 keV in ^{195}Pt. It is interesting to note that the sum of the (d,p) and (d,t) spectroscopic factors for these two positive parity states is still much smaller than the value $(2j+1)/2$ predicted by the simple shell model. On the other hand, they are larger than unity, the maximum value consistent with the simple Nilsson model.[14] This situation, peculiar to transitional nuclei, has been explained in terms of Coriolis coupling in the iridium isotopes and in ^{195}Pt.[1,18] It is probable that the $\frac{13}{2}^+$ state is the head of a decoupled band based on an $i_{13/2}$ hole state similar to that observed in the lighter platinum isotopes.[3]

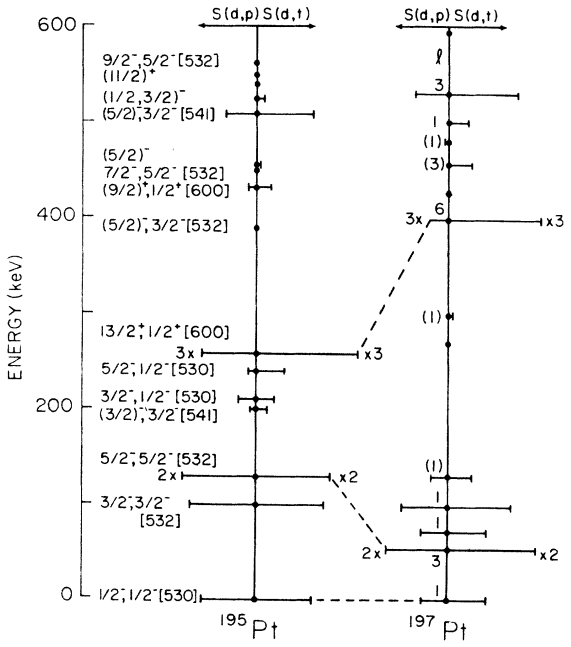

FIG. 6. Comparison between the states of ^{195}Pt and ^{197}Pt below 600 keV. The lengths of bars represent the spectroscopic factors. Nilsson assignments are shown for ^{195}Pt and l assignments for ^{197}Pt.

Serious problems arise for the interpretation of the $l=1$ states in ^{197}Pt. In the present (d,p) and (d,t) experiment, four relatively strong peaks at 0, 72, 99, and 131 keV were assigned as $\frac{1}{2}^-$ or $\frac{3}{2}^-$. The latter two states, previously unknown, were also populated through primary transitions from the thermal neutron capture. It is not probable that any of these $l=1$ states is a rotational band member based on the ground state, since the $\frac{3}{2}^-$ member of the ground $\frac{1}{2}^-[530]$ band lies at 211 keV in ^{195}Pt. Possible candidates for the assignments might be the $\frac{1}{2}^-[530]$, $\frac{3}{2}^-[532]$, $\frac{3}{2}^-[541]$, and $\frac{1}{2}^-[541]$ Nilsson states. However, the large single-particle strengths observed for all of the four states reject the $\frac{3}{2}^-[541]$ and $\frac{1}{2}^-[541]$ assignments which are predicted by the Nilsson model to have small spectroscopic factors. This prediction is supported by the fact that only the $\frac{1}{2}^-[530]$ and $\frac{3}{2}^-[532]$ Nilsson states among these candidates are strongly populated in ^{195}Pt (see Fig. 6).

It is also possible that four low-lying $l=1$ states can be understood in terms of collective $|K-2|$ excitations built upon the $\frac{1}{2}^-[530]$ and $\frac{3}{2}^-[532]$ states. It is expected that collective $\{\frac{1}{2}^-[530], 2^+\}\frac{3}{2}^-$ and $\{\frac{3}{2}^-[532], 2^+\}\frac{1}{2}^-$ states can contain appreciable admixtures of the $\frac{3}{2}^-[532]$ and $\frac{1}{2}^-[530]$ Nilsson states, respectively, via particle-vibration coupling. Together with the two Nilsson states, the two $|K-2|$ states would account for four low-lying $l=1$ states that would be populated via the neutron transfer reaction. However, if there is a strong interaction between two states with

the same spin and parity, it is difficult to understand how these two states occur in such close energy proximity as the low-lying $l=1$ states observed in ^{197}Pt. Collective $|K-2|$ excitation and particle-vibration coupling in the rotation-vibration model[4] correspond to rotational excitation around the third axis and coupling of particle motion to the asymmetric deformation in the asymmetric rotator model.[19] Thus, similar difficulties can be expected to arise in understanding this nucleus on the basis of either model. In fact attempts to understand the properties of four low-lying $l=1$ states in terms of the rotation-vibration model[4] or asymmetric rotator model[19] were not successful. These calculations used methods described previously[1] and parameters consistent with the spectroscopic data[12,13] of the neighboring even-even ^{196}Pt nucleus ($\beta \cong -0.13, \hbar/2\vartheta_0 = 36.3$ keV and $E_\gamma = 405$ keV for the rotation-vibration model and $\beta \cong 0.14, \gamma = 30°$ and $\hbar^2/2\vartheta_0 = 39.6$ keV for the asymmetric rotator model).

In this connection, it is interesting to note that apparent $|K_0 - 2|$ excitations occur at surprisingly low excitation energies in the iridium isotopes (82 keV in ^{191}Ir and 73 keV in ^{193}Ir).[18,20-22] Simple particle-vibration coupling also could not provide a satisfactory explanation for the properties of these states.[18]

Calculations of potential energy surfaces show only shallow minima in the β and γ plane for the transitional platinum isotopes.[23] This suggests that different core excitation modes may occur by adding one quasiparticle in a different orbital. This effect is not included in coupling of one quasiparticle to a vibrator or an asymmetric rotator. Thus, the difficulty in understanding properties of four low-lying $l=1$ states of ^{197}Pt in terms of the Nilsson model,[14] rotation-vibration model,[4] or asymmetric rotator model[19] would indicate that this kind of dynamic coupling effect may be important in describing the nuclear structure of ^{197}Pt.

After this work was completed we received a report of a paper[24] in which the ^{198}Pt$(p,d)^{197}$Pt reaction was studied. In that work 15 levels between the ground state and 748 keV were observed. The l values of the first seven levels (all that were reported) and the approximate energies of all 15 levels are in agreement with our observations.

ACKNOWLEDGMENTS

We are grateful to R. Leonard for preparing the targets, to R. Lasijo, R. Bagnell, C. Atwood, and M. Hoehn for assistance in taking the charged particle reaction data and L. Wright and R. Schendel for scanning the plates. We also thank E. T. Jurney and the staff of the Los Alamos Omega West reactor for making the (n,γ) experiments possible. We would like to thank J. A Cizewski and R. F. Casten for providing us with their ^{195}Pt$(n,\gamma)^{196}$Pt data prior to publication.

---

*Supported by U. S. DOE and by the NSF on Grant No. PHY 77-12876.

†Present address: Los Alamos Scientific Laboratory, Los Alamos, New Mexico 87545.

[1] Y. Yamazaki and R.K. Sheline, Phys. Rev. C 14, 531 (1976).

[2] J. E. Glenn, R. J. Pryor, and J. X. Saladin, Phys. Rev. 188, 1905 (1969).

[3] M. Piiparinen, J. C. Cunnane, P. J. Daly, C. L. Dors, F. M. Bernthal, and T.L. Khoo, Phys. Rev. Lett. 34, 1110 (1975); S. K. Saha, M. Piiparinen, J. C. Cunnane, P. J. Daly, C. L. Dors, T. L. K. Khoo, and F. M. Bernthal, Phys. Rev. C 15, 94 (1977).

[4] A. Faessler and W. Greiner, Z. Phys. 168, 425 (1962); 170, 105 (1962); 177, 190 (1964).

[5] B. Harmatz, Nucl. Data Sheets 20, 73 (1977).

[6] P. Mukherjee, Nucl. Phys. 64, 65 (1965).

[7] C. P. Browne and W. W. Buechner, Rev. Sci. Instrum. 27, 899 (1956).

[8] A. H. Wapstra and K. Bos, At. Data Nucl. Data Tables 19, 215 (1977).

[9] P. D. Kunz, computer program DWUCK, University of Colorado (unpublished).

[10] E. T. Jurney, H. T. Motz, and S. H. Vergors, Jr., Nucl. Phys. A94, 351 (1967).

[11] R. C. Greenwood and R. G. Helmer, Nucl. Instrum. Methods 121, 385 (1974).

[12] J. A. Cizewski and R. F. Casten, private communication; J. A. Ciweski, R. F. Casten, G. J. Smith, M. L. Stelts, W. R. Kane, H. J. Börner, and W. F. Davidson, Phys. Rev. Lett. 40, 167 (1978).

[13] M. R. Schmorak, Nucl. Data Sheets B7, 395 (1972).

[14] S. G. Nilsson, K. Dan Vidensk. Selsk. Mat. Fys. Medd. 29, No. 16 (1955).

[15] At the spherical limit the Nilsson states labeled by the oblate asymptotic quantum numbers $\frac{5}{2}^-[532]$, $\frac{3}{2}^-[532]$, $\frac{1}{2}^-[530]$, $\frac{3}{2}^-[541]$, $\frac{1}{2}^-[541]$, $\frac{1}{2}^+[600]$, $\frac{9}{2}^+[615]$ correspond to those labeled by the prolate asymptotic quantum numbers $\frac{5}{2}^-[503]$, $\frac{3}{2}^-[512]$, $\frac{1}{2}^-[521]$, $\frac{3}{2}^-[501]$, $\frac{1}{2}^-[510]$, $\frac{1}{2}^+[660]$, and $\frac{9}{2}^+[615]$, respectively.

[16] G. Andersson, S. E. Larsson, G. Leander, P. Möller, S. G. Nilsson, I. Ragnarsson, S. Aberg, B. Bengtsson, J. Dudek, B. Nerlo-Pomorska, K. Pomorski, and S. Szymanski, Nucl. Phys. A268, 205 (1976).

[17] B. R. Mottelson and S. G. Nilsson, Mat. Fys. Skr. Dan. Vid. Selsk. 1, No. 8 (1959).

[18] Y. Yamazaki, R. K. Sheline, and D. G. Burke, Z. Phys. A285, 191 (1978).

[19]A. S. Davydov and G. F. Fillipov Nucl. Phys. 8, 237 (1958).
[20]R. H. Price and M. W. Johns, Nucl. Phys. A187, 641 (1972).
[21]P. Norgaard, K. M. Bisgaard, K. Gregersen, and P. Morgan, Nucl. Phys. A162, 449 (1971).
[22]R. H. Price, D. G. Burke, and M. W. Johns, Nucl. Phys. A176, 338 (1971).
[23]K. Kumar and M. Baranger, Nucl. Phys. 110, 529 (1968).
[24]G. Berrier-Ronsin, M. Vergnes, G. Rotbard, J. Vernotte, J. Kalifa, R. Seltz, and H. L. Sharma, preprint 1977.